Chapter 48

LARGE SCALE STATIC AND DYNAMIC FRICTION EXPERIMENTS

By Khosrow Bakhtar and Nick Barton

Senior Engineer, Terra Tek Engineering
Salt Lake City, Utah

Director of Geomechanics, Terra Tek Engineering
Salt Lake City, Utah

ABSTRACT

A series of nineteen shear tests were performed on fractures 1 m^2 in area, generated in blocks of sandstone, granite, tuff, hydro-stone and concrete. The tests were conducted under quasi-static and dynamic loading conditions. A vertical stress assisted fracturing technique was developed to create the fractures through the large test blocks. Prior to testing, the fractured surface of each block was characterized using the Barton JRC-JCS concept. The results of characterization were used to generate the peak strength envelope for each fractured surface. Attempts were made to model the stress path based on the classical transformation equations which assumes a theoretical plane, elastic isotropic properties, and therefore no slip. However, this approach gave rise to a stress path passing above the strength envelope which *is* clearly unacceptable. The results of the experimental investigations indicated that actual stress path is affected by the dilatancy due to fracture roughness, as well as by the side friction imposed by the boundary conditions. By introducing the corrections due to the dilation and boundary conditions into the stress transformation equation, the fully corrected stress paths for predicting the strength of fractured blocks were obtained.

INTRODUCTION

An experimental test program was devised to study the shear strength of rock joints. The large size of the samples (1 m^2) was designed to extend the data base beyond the usual limitations of laboratory test equipment. Attempts were also made to compare the shear strength under pseudo static and dynamic rates of shear. The tests were performed on large fractured blocks of sandstone, tuff, granite, hydrostone and concrete. The large fractured surfaces were

generated by slowly driving a "V"-shaped steel bar into a shallow saw-cut on the top surface of the 1.5 ton blocks of rock, while simultaneously applying a vertical stress of 6.9 MPa across the whole block using triangular-shaped flatjacks. The fractures were effectively controlled by their propagation parallel to the principal stress.

The simulated joint surfaces (fracture surfaces) created in the large blocks were characterized using the method developed by Barton and Choubey (1977). The method consisted of measuring the compression strength of the joint walls (JCS) as well as the intact rock (σ_c), taking small scale roughness profiles from the joint surface, and converting these small scale parameters to the full scale prototype using the scaling relationships developed by Barton and Bandis (1982). Tilt tests were performed on the large fractures to determine JRC , and on the planar, wire sawn surfaces of the same blocks of rock to determine the basic angles of friction (ϕ_b) • These parameters were used to generate peak shear strength envelopes under a range of effective normal stress levels using the following equation:

$$\tau = \sigma_n' \tan [(\phi_b + JRC_n \log (JCS_n / \sigma_n'))] \qquad (1)$$

Where: τ = peak sher strength

σ_n' = effective normal stress across joint

ϕ_b = basic friction angle = ϕ_r (residual) when no weathering

JRC_n = Joint Roughness Coefficient (full scale)

JCS_n = Joint Wall Compression Strength (full scale)

From the nineteen shear tests conducted, half the tests were performed under conditions of pseudo-static loading, using flatjacks to simulate the biaxial states of stress. The remaining half of the tests were performed at dynamic rates of loading, with peak axial loads of up to 2670 KN applied in 80 to 90 milliseconds, using a high pressure gas loading system. Figure 1 shows the overall view of the biaxial frame as well as the dynamic actuator used for this investigation.

ANALYSIS BASED ON QUASI-STATIC DATA

In the initial stages of analysis, attempts were made to analyze the data based on the two dimensional theory of elasticity. In this method, it is assumed that the normal and shear components across the fracture can be determined from the classical transformation equations in which no slip is assumed to occur (i.e. an imaginary shear plane inclined at angle p to the principal stress):

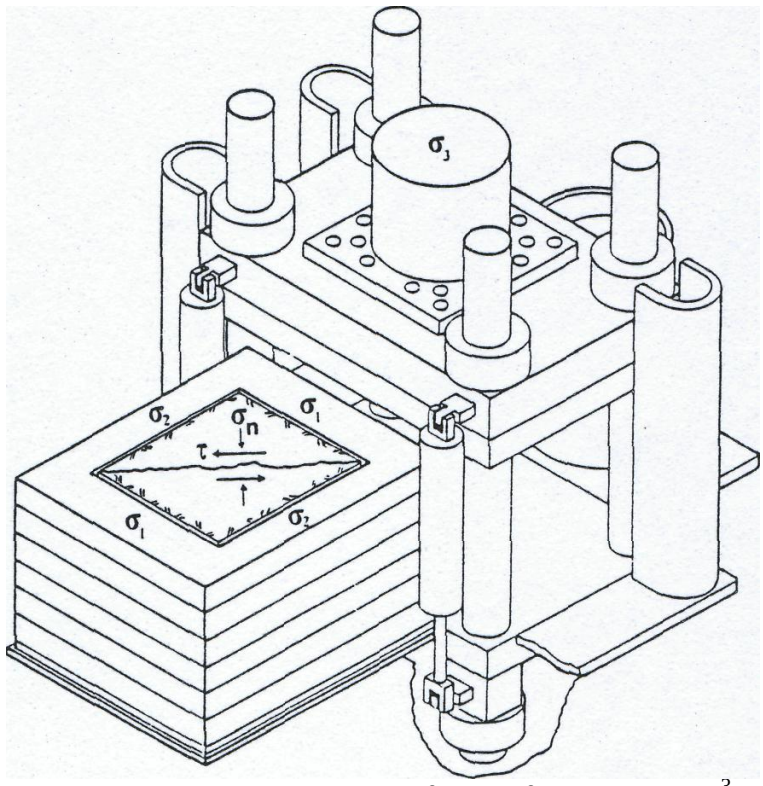

Fig. 1. Terra Tek's polyaxial cube test facility for loading 1 m^3 blocks of intact or jointed rock. Horizontal stresses σ_1 and σ_2 are applied by flat jacks, with a maximum rating of 35 MPa in each direction. Dynamic loads are applied by the (σ_3) cylinder using gas loading. The fracture is rotated 90° for these tests, and is unconfined.

$$\sigma_n = \tfrac{1}{2}(\sigma_1 + \sigma_2) - \tfrac{1}{2}(\sigma_1 - \sigma_2)\cos 2\beta \qquad (2)$$

$$\tau = \tfrac{1}{2}(\sigma_1 - \sigma_2)\sin 2\beta \qquad (3)$$

However, due to fracture dilation during shear causing out-of-plane shear, and due to end friction effects, the above equations overestimate the applied value of shear stress along the fracture surface, and cannot therefore be used in their existing forms.

An improved method of analysis was developed in which the contribution or the effects of dilation and side friction were introduced into the transformation equations. These effects are illustrated schematically by the various force diagrams shown in Figure 2.

To account for the dilation effect, the mobilized joint roughness coefficient JRC(mobilized) was computed from Equation 4 and the mobilized dilation angle (d_n°) was calculated using Equation 5, after Barton and Bakhtar (1983).

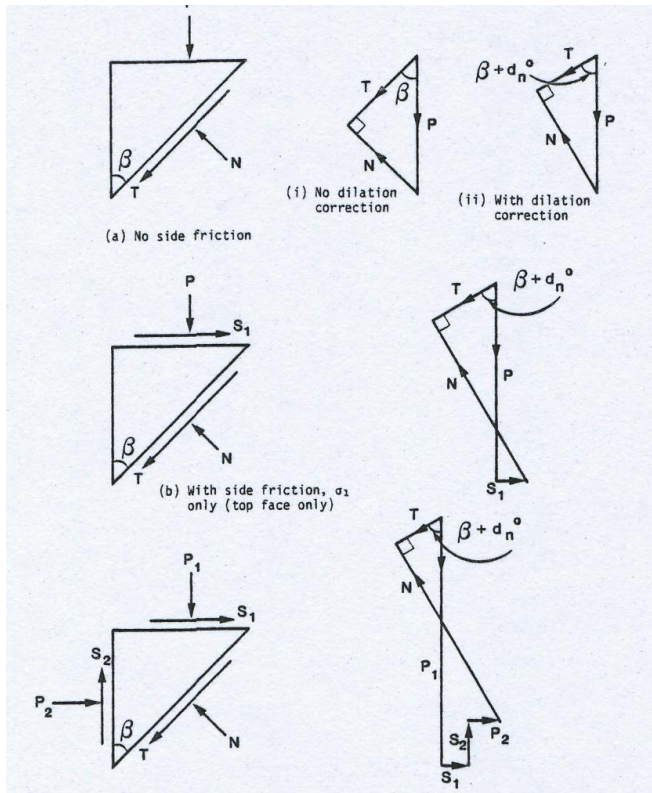

Fig. 2. Force diagrams showing the contribution of dilation and side friction to the transformation equations.

$$\text{JRC(mobilized)} = [\tan^{-1}\left(\frac{\tau(mobilized)}{\sigma_{n'}}\right) - \phi_r] - [\log\frac{JCS_n}{\sigma_{n'}}]^{-1} \quad (4)$$

$$d_n°\text{(mobilized)} = \frac{1}{2}\,\text{JRC(mobilized)} - [\log\frac{JCS_n}{\sigma_{n'}}] \quad (5)$$

where : $d_n°$ = dilation angle
(the term "mobilized" indicates as intermediate value, either pre- or post-peak.)

To account for the dilation effect $d_n°$ was added to β in Equations 6 and 7 as shown below:

$$\sigma_n = ½(\sigma_1 + \sigma_2) - ½(\sigma_1 - \sigma_2)\cos 2(\beta + d_n°) \quad (6)$$

$$\tau = ½(\sigma_1 - \sigma_2)\sin 2(\beta + d_n°) \quad (7)$$

The effect of side friction is accounted for by the following equations:

$$\left.\begin{aligned} S_2 &= \mu P_2 \\ S_1 &= \mu P_1 \end{aligned}\right\} \qquad (8)$$

where μ is the friction of the steel-teflon interface. These forces are shown in Figure 2. A series of tests was conducted to determine the friction between Teflon and steel. An average value of 10° was obtained. This results in a value of 0.176 for μ.

For the general case (Figure 2c) where there is friction on the four loaded sides of the block, the σ_1 and σ_2 terms are replaced by $(\sigma_1 - \mu\sigma_2)$ and $(\sigma_2 + \mu\sigma_1)$. Substitution of the above into Equations 6 and 7 results in the final expressions given below:

$$\sigma_n = \tfrac{1}{2}\{(\sigma_1 + \sigma_2) + \mu(\sigma_1 - \sigma_2)\} - \{(\sigma_1 - \sigma_2) - \mu(\sigma_1 + \sigma_2)\}\cos 2(\beta + d_n°) \qquad (9)$$

$$\tau = \tfrac{1}{2}\{(\sigma_1 - \sigma_2) - \mu(\sigma_1 + \sigma_2)\}\sin 2(\beta + d_n°) \qquad (10)$$

The intercept of this modified stress path with the strength envelope given by Equation 1 defines the theoretical failure strength of the fracture surface. In this way, prior to conducting any shear test on a fractured block, one should be able to define the stress level at which the shear failure is expected to occur.

For most of the quasi-static experiments conducted, the test samples were instrumented by means of three displacement transducers, two perpendicular to the fracture, sensing dilation, and one along the fracture, sensing shear displacement. Two pressure transducers mounted on the flatjacks were also used to monitor the stress field. The following data was derived and plotted:

shear stress versus shear displacement,
dilation versus normal stress,
dilation versus shear displacement

DYNAMIC SHEAR TESTS

In the case of the dynamic tests, the fractured blocks of rock were rotated 90° relative to the position shown in Figure 1. The fractures were therefore set with a predetermined dip, which could be made steeper or shallower by means of specially cast gypsum wedges placed under the blocks. The wedge angle was varied according to the roughness of the fracture, so that

reasonably high loads would be reached before shear failure occurred. Load was applied by dumping high pressure helium from the bottom of the cylinder depicted in Figure 1.

The following dynamic data was acquired and plotted:

- applied load versus rise time
- shear stress versus shear displacement
- normal stress versus dilation
- dilation versus shear displacement
- shear displacement versus rise time
- normal stress versus shear displacement

In general shear velocities in the range 400-4000 mm/sec were reached, rise times to peak loads varied from 15 to 90 milliseconds, and maximum loads as high as 270 tons were reached. These rise times and shear velocities are broadly representative of conditions to which deep based tunnel structures might be subjected. However, due to the size of the samples, stress levels were relatively low.

TYPICAL RESULTS

Examples illustrating the effects of dilation and end friction correction on large scale block tests are given in this section. Figure 3 shows the strength envelope with the associated stress paths for a typical static test on a large fractured block. The fracture in this example (sandstone No. 7) did not shear, even when a flatjack pressure of 28.7 MPa was reached, at which point the block failed in compression. The correction for boundary effects is insufficient on its own to account for this failure to shear; likewise the dilation correction. However, when combined, the fully corrected stress path No. 3 does fall beneath the envelope and explain why shear did not occur.

Figure 4 illustrates the corrected path obtained for a typical dynamic test. For the case of this granite sample (#13) the dilation corrected path predicted the failure strength to within 15 percent of the actual value. In this test the peak load was 267 tons, the rise time 91 msecs, and the peak shear velocity was 4210 mm/sec. The corresponding peak acceleration was 58.3 g.

DISCUSSION

The nineteen large scale friction tests performed under this study are probably unique in terms of sample size and load levels. Fracture areas of approximately 1 m^2 were subjected to loads as high as 2700 tons in pseduo-static tests using flatjacks, and to loads as high as 270 tons in dynamic tests. In the latter, rise times as fast as 15 milliseconds have been achieved, with maximum shear velocities along the fractures of 4 meters/second, and corresponding maximum acceleration of 60 g.

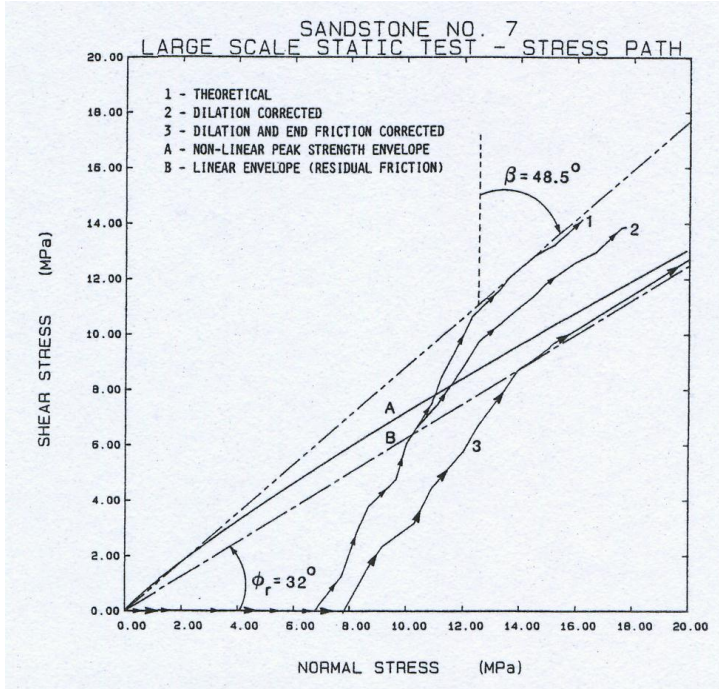

Fig. 3. Corrected stress paths to account for out-of-plane dilation (envelope 2) and side friction (envelope 3) explain the failure to shear this fractured sandstone block.

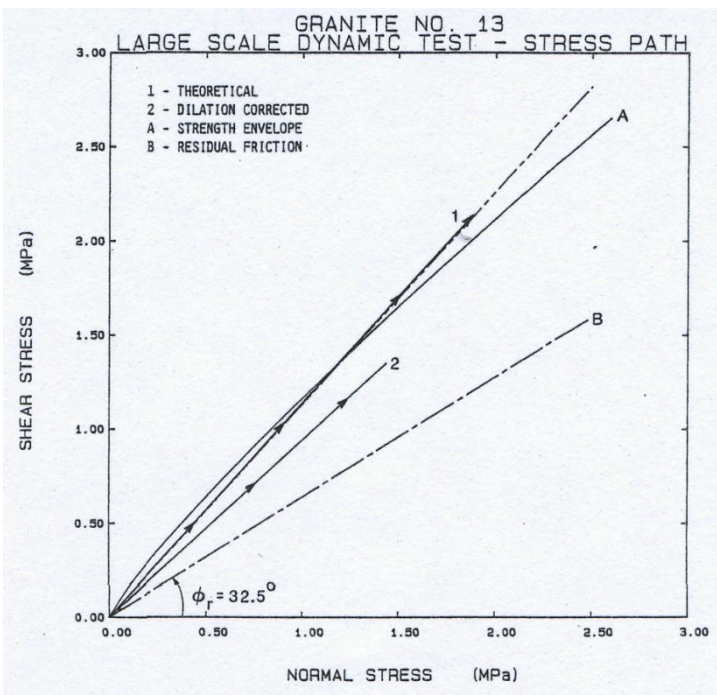

Fig. 4. Strength envelope with the associated stress paths for large fractured granite block, sample *#13*.

Prior to testing in pseudo-static or dynamic shear, each fracture or saw cut was characterized by performing: 1) tilt tests for JRC, 2) Schmidt hammer tests for JCS, 3) tilt tests for ϕ_b , and 4) roughness profile measurements. The data obtained was used as input in our joint behavior model to predict: peak shear strength envelope (τ, and σ_n) and dilation (d_n) due to JRC(mobilized). The latter was used to correct the theoretical (transformed) stress path to allow for out of plane shear (at angle $\beta + d_n$). When shearing commences and the normal stress also increases, the dilation angle will change successively, becoming smaller at higher stress. A further correction was made for end friction effects, which are strictly a function of the test method used, and which would not be applied in-situ where natural far-field boundaries exist.

In general, utilization of the characterization data and the above dilation and friction correction allowed us to predict the subsequently measured strengths to an accuracy of ±15%. When the tests were partitioned as pseudo-static or dynamic, the average predicted shear strengths were approximately 5% lower than measured under pseudo-static conditions, and 10% lower than measured under dynamic conditions. By implication, the joint behavior model is slightly conservative, and the dynamic strength may be some 5% higher than the static strength when shear displacement velocities of approximately 0.001-0.1 mm/sec (pseudo-static) are compared with the dynamic velocity range of approximately 400-4000 mm/sec.

A review of test data indicates that the compressive strength of rock does increase significantly as loading rate is increased. For example, tests reported by Green and Perkins (1968) indicate approximately 40% increase in σ_c(unconfined) when the strain rate is increased from about 10^{-4} sec^{-1} to 10^3 sec^{-1}.

Under conditions of shear loading our test results indicate only minor rate effects (approximately 5%) when shear velocities are no more than 1-4 meters per second. Cyclic shear loading tests reported by Gillette, et al. (1983) for tension fractures in sandstone indicate that rate dependence is probably absent until velocities exceeding 1 mm/second are reached. Between 1 mm/sec and 100 mm/sec an increase in shear strength of 10-15% was indicated. However, it is not known exactly how comparable rate effects obtained from cyclic loading will be, compared to the single pulse, unidirectional shear events in the present series of tests.

The fracture surface profiles shown in Figure 5 illustrate the manner in which surface morphology is related to the JRC value obtained from large scale tilt tests. In the nineteen tests, the following average values were obtained for the laboratory and full scale shear strength parameters.

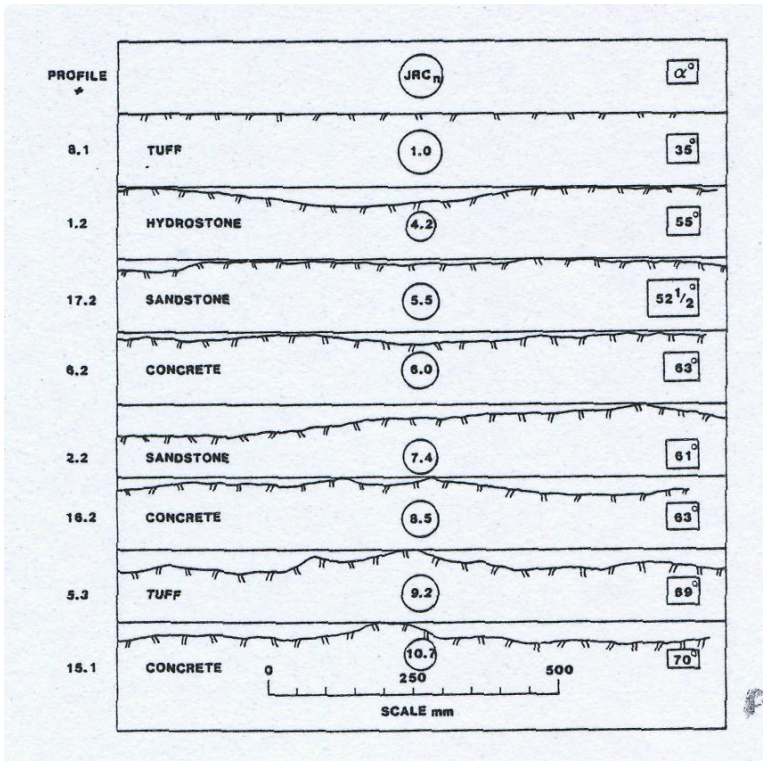

Fig. 5. Fracture surface profiles showing relationship between JRC , tilt angle a°, and surface morphology. The data was obtained by conducting tilt tests (self weight shear) on the 1% ton blocks.

TABLE 1. Average Laboratory and Full-Scale Shear Strength Parameters Obtained in This Study

Laboratory Scale	Full-Scale
JCS_O = 52 MPa	JCS_n = 30 MPa
JRC_O = 7.9	JRC_n = 5.6
ϕ_r = 32°	ϕ_r = 32°

For illustrative purposes we will utilize the above average values to demonstrate the approximate differences that are obtained when laboratory data is used to predict shear strength in place of in-situ scale data. We will further demonstrate the effect on in-situ shear strength that is predicted, if a 50% increase in compressive strength is assumed to occur as a result of dynamic loading. Three effective normal stress levels will be utilized: 1 MPa, 10 MPa and 30 MPa. These results demonstrate that the parameters affecting shear strength can be classed in order of importance as follows:

TABLE 2. Demonstration of Scale Effects and Dynamic Load Effects

Normal Stress	Laboratory Scale (Static)		In-Situ Scale (Static)		In-Situ Scale (Dynamic)	
	τ (MPa)	ϕ (peak)	τ (MPa)	ϕ (peak)	τ (MPa)	ϕ (peak)
1 MPa	1.02	45.6°	0.85	40.3°	0.88	41.3°
10 MPa	7.72	37.7°	6.92	34.7°	7.18	35.7°
30 MPa	20.15	33.9°	18.75	32.0°	19.47	33.0°

First Order -- normal stress level
Second Order -- scale effect
Third Order -- dynamic loading

A dynamic event causing an increase in normal stress will obviously result in a very large increase in shear resistance. If, for some reason, the dynamic event left the normal stress level unchanged, then little increase in shear strength could be expected. The 50% increase in compressive strength assumed above results in only 3-4% increase in peak shear strength, due to the logarithmic dependence of the friction angle on the ratio of JCS/σ_n .

ACKNOWLEDGEMENTS

The authors are indebted to the Defense Nuclear Agency for funding this project. We are also indebted to Alan Black, Dick Lingle, Mohamad Khodaverdian, Scott Woodhead and Paul Schweadiman of Terra Tek for their invaluable support.

REFERENCES

Barton, N. and Bandis, S., 1982, "Effects of Block Size on the Shear Behavior of Jointed Rock," Keynote Lecture, 23rd U.S. Symposium on Rock Mechanics, Berkeley, California.

Barton, N. and Choubey, V., 1977, "The Shear Strength of Rock Joints in Theory and Practice," Rock Mechanics, Vol. 10, pp. 1-54.

Barton, N. and Bakhtar, K. , 1983, "Bolt Design Based on Shear Strength," International Symposium on Rock Bolting, Abisco, Sweden.

Gillette, D.R., Sture, S., and Ko, H-Y., 1983, "Dynamic Behavior of Rock Joints," Preprint 24th Symposium on Rock Mechanics, Texas A&M University.

Green, S.J., and Perkins, R.D., 1968, "Uniaxial Compression Tests at Varying Strain Rates on Three Geologic Materials," 10th U.S. Symposium on Rock Mechanics, University of Texas, Austin.